

Response Surface Methodology for Optimizing Cd(II) Adsorption onto a Novel Chemically Changed Nano Zn₂Al-Layer Double Hydroxide

Mohtaram Janighorban^a, Nahid Rasouli^{a,*}, Nasrin Sohrabi^a, Mehrorang Ghaedi^b

^a Department of Chemistry, Payame Noor University, P.O. Box 19395-3697, Tehran, Iran

^b Chemistry Department, Yasouj University, Yasouj 75918-74831, Iran

ARTICLE INFO

Received: 07 March 2020
Revised: 07 April 2020
Accepted: 26 April 2020
Available online: 29 April 2020

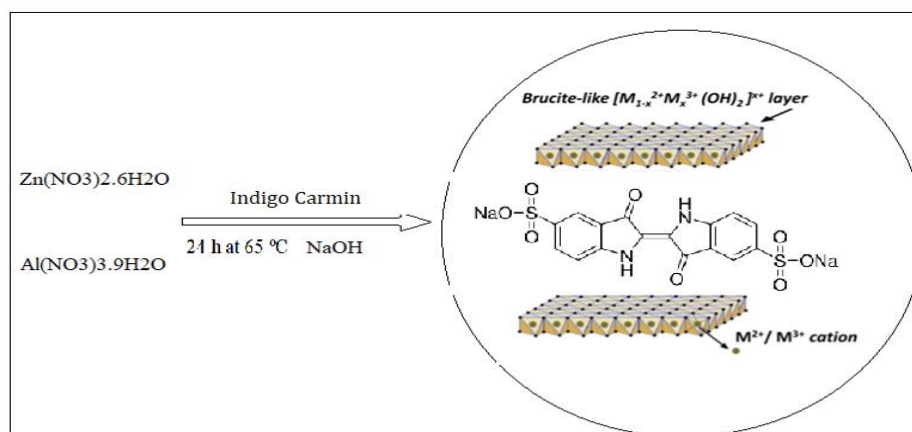
KEYWORDS

Nano-layered double hydroxide
Optimization
Central composite design (CCD)
Response surface methodology (RSM)

ABSTRACT

In this work, a novel chemically adsorbent based on Zn₂Al-layered double hydroxide (LDH) that modified by indigo carmine (IC) (Zn₂Al-LDH/IC) was synthesized. The chemical composition and morphology of the synthesized Zn₂Al-LDH/IC were investigated using the X-ray diffraction (XRD), Brunauer-Emmett-Teller (BET), field emission scanning electron microscopy (FE-SEM), and energy-dispersive X-ray spectroscopy analysis. Response surface methodology (RSM) using the central composite design (CCD) is applied to optimize the adsorption process parameters for Cd(II) removal from the aqueous solution using a novel chemically modified nano Zn₂Al-layered double hydroxide (Zn₂Al-LDH/IC). The combined effect of adsorption parameters such as contact time, initial Cd(II) concentration, adsorbent amount and initial pH of solution were studied. The results obtained by ANOVA analysis displayed the relative significance of the process parameters in the adsorption process. The optimum conditions to remove Cd(II) from aqueous solution were at the initial Cd(II) concentration of 52 mg/L⁻¹, pH 4.13, the adsorbent dose 0.06 g, temperature of 36.5 °C and contact time 36 min. In optimum conditions, high adsorption efficiency and maximum adsorption capacity were 47.3% and 6.11 mg/g, respectively. Adsorption of Cd(II) by nano Zn₂Al-LDH/IC could be well examined with Langmuir and Freundlich isotherms and the pseudo second-order kinetic model was fitted to the adsorption kinetic data. Furthermore, the thermodynamic data exhibited that the adsorption process of Cd(II) by nano Zn₂Al-LDH/IC was spontaneously and exothermic.

GRAPHICAL ABSTRACT



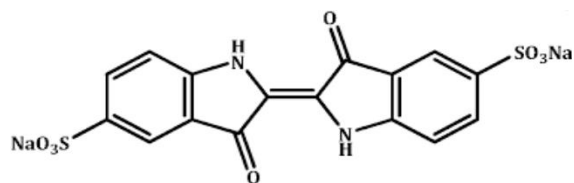
* Corresponding author's E-mail address: n.rasooli55@yahoo.com, nara110@yahoo.com

Introduction

Recently, the rapid increase in industrial activity has prompted heavy metal contamination in the environment. These heavy metals are not eco-friendly and toxic [1,2], consequently heavy metals in trace extents may induce high danger to human health and can cause major hurt to plants, animals and humans. Cadmium is one of the toxic heavy metals that, causing the environmental pollution [3-5]. Therefore, it is essential to remove the Cd(II) ions from aqueous solutions. Up to now, there have been various methods developed to eliminate heavy metals from aqueous environments [6-11]. From among these methods, adsorption method has advantages such as non-hazardous, economic view point, flexibility in design, high selectivity and environmentally friendly, which differentiate it from other technologies [12-16]. Layered double hydroxides (LDHs) or hydrotalcite-like compounds recognized as the anionic clay have become a major type of adsorbents owing to many applications such as super capacitors [17,18], catalysis [19,20], drug delivery [21,22] wastewater management [23-26] and flame retardant epoxy formulation [27]. Particularly, their applications as adsorbents have extreme consideration due to their low cost, high surface area, highly tunable interior architecture [28], non-toxicity [29,30] and changeable anionic properties. Layered double hydroxide have the general formula $[M_{1-x}^{II}M_x^{III}(\text{OH})_2]^{x+}[A_n]_{x/n}.m\text{H}_2\text{O}$, where M^{II} and M^{III} which show a divalent and a trivalent cation, respectively, A_n is the interlayer anion, such as CO_3^{2-} , Cl^- and NO_3^- , located in the interlayer and the lamellar surface. In recent years, surface-modified adsorbents have been increasingly utilized for heavy metal removal

from aqueous environments. Earlier research revealed that, the LDH intercalated with amino acids [31], ethylene diamine tetra acetic acid [32], glutamate [33], and di ethylene tri-amine penta acetate and meso-2,3-dimercaptosuccinate [34], possessed a higher tendency to toxic metal cations than the original LDH adsorbents. Consequently, modification with indigo carmine (IC) as a food coloring for Cd (II) adsorption is estimated to increase the adsorption yield. Response surface methodology (RSM) combined with central composite design (CCD) is one of the most used optimization methods [35]. RSM is a statistical and mathematical algorithm that is used to detect the effect of several parameters affecting the experimental results at the same time. The main advantage of using the RSM for adsorption is that it decreases the number of experimental replications required to estimate the various parameters and their interactions. The statistical design can help to simplify the interaction of the various factors and determine the optimum condition of the variables for adsorption process. CCD is ideal for successive trials, providing a sufficient amount of information for testing lack of fit while not confusing an unusually large number of design points. In the current research study, the main goal is to synthesize a novel chemically modified adsorbent ($\text{Zn}_2\text{Al-LDH/IC}$) for the removal of Cd(II) from aqueous solution and optimization of several operational adsorption parameters using central composite design (CCD) combined with response surface methodology (RSM). To the best of our knowledge, there is has been no study conducted on the synthesis of the $\text{Zn}_2\text{Al-LDH/IC}$ and use it as an adsorbent for the Cd^{2+} removal applying response surface methodology (RSM) modeling.

Scheme 1. Chemical structure of Indigo carmine



Experimental

Materials and instrumentation

All the materials were commercial reagent grade and purchased from the Merck and Sigma Aldrich. The Cd²⁺ concentration was determined using the atomic absorption spectrometer, Specter AA 220, VARIAN. Magnetic stirrer and water bath were IKA, big-squid [ocean], and Julabo F12-MP, (from Germany), respectively. The analysis of the samples performed using the powder X-ray diffraction (Holland Philips X-pert, X-ray diffractometer with Cu-K α radiation). The particle size, exterior morphology and analysis of elements in the samples characterized using the scanning electron microscopy (JEOL JEM-3010 SEM) and the BET analysis was accomplished using BELSORP Mini II instrument. A digital pH Burret 24, CRISON (PANIA) was employed for adjusting.

Preparation of Zn₂Al-LDH modified with indigo carmine (IC)

The Zn₂Al-layered double hydroxide (LDH) modified with indigo carmine (IC) (Zn₂Al-LDH/IC) was prepared by the co-precipitation method [36]. At the first step, the carbon dioxide free (CO₂-free) solution was prepared by flowing the N₂ into the deionized water for 30 min at 60 °C and used through the synthesis procedure. In this manner, a mixture of Zn(NO₃)₂·6H₂O (5.2 g, 0.018 mol) and Al(NO₃)₂·9H₂O (3.2 g, 0.008 mol) with Al to Zn molar ration (1:2) and indigo carmine (5.07 g, 0.028 mol) in 250 mL deionized water was added to a solution of NaOH (1M) under the constant stirring until reaching pH=10-11, then continue flowing N₂ into solution at 60 °C to complete the precipitation process. Then, the achieved product stirred for 24 h at 65 °C. The obtained product was washed thoroughly with doubly distilled water. Then, the washed sample was dried at room temperature.

Adsorption studie

The Cd²⁺ concentrations were determined according to common traditional flame atomic absorption spectrometry, at the wavelength of 228.8 nm, standard working concentration of 0.25, 0.5, and 1.0 ppm and fuel acetylene. The efficiency of Cd²⁺ elimination was determined at different experimental conditions identified according to the CCD method. The adsorption capacity for the Cd²⁺ uptake, q_e (mg/g), at the equilibrium can be determined by the subsequent Equation 1.

$$q_e = \frac{(C_i - C_e)V}{m} \quad (1)$$

Where C_i and C_e (mg/L) refer to cadmium concentrations at the initial and equilibrium conditions, respectively; V (L) is the cadmium solution volume, and m (g) is the adsorbent mass. In the kinetic study, Cd²⁺ adsorption amount (q_t) can be considered by Equation 2.

$$q_t = \frac{(C_0 - C_t)}{C_0} \times 100 \quad (2)$$

Where C_i and C_t (mg/L) are the Cd²⁺ concentration at the initial and time t , respectively. V (L) is the Cd²⁺ solution volume, and m (g) is the Zn₂Al-LDH/IC adsorbent mass.

Design of experiment

The design of experiment technique is one of the most popular techniques used to determine and control the effective factors and to optimize and attain the favorable conditions of a given process [37]. Based on the statistical approaches (depending on the problem under study), design of experiment recognizes the effective parameters and reduces the uncontrollable factors. Response surface methodology (RSM) is one of the most proper and commonly used methods in designing the experiments. The RSM technique is a combination of statistical techniques for experimental modeling and

optimization of the process parameters, in which the desired answer is affected by a number of independent variables [38–40]. With this statistical design, the number of experiments reduces and all the coefficients of quadratic regression model and the interaction factors can be measured. In the RSM method, a model is defined for each independent variable through which the main

and the interacting effects of the factors are expressed on each separate variable, and the multivariate model is written as Equation 3 [41].

$$(Y)\% = \beta_0 + \sum_{i=1}^n \beta_i X_i + \sum_{i=1}^n \beta_i X_i^2 + \sum_{i=1}^{n-1} \sum_{j=2}^n \beta_{ij} X_i X_j + \varepsilon \tag{3}$$

Table 1. Levels of factors in CCD

Factors	Unit	Symbol	-α	levels			+α	Std.Dev.
				Low Actual	Mean	High Actual		
Concentration (C)	Mg/L ⁻¹	A	-1	35.00	57.500	80.00	+1	19.486
pH		B	-1	4.00	6.500	9.00	+1	2.165
adsorbent mass(m)	g	C	-1	0.027	0.046	0.064	+1	0.016
Contact time(time)	min	D	-1	35.00	60.00	85.00	+1	21.651
Temperature (T)	°C	E	-1	20.00	30.00	40.00	+1	8.660

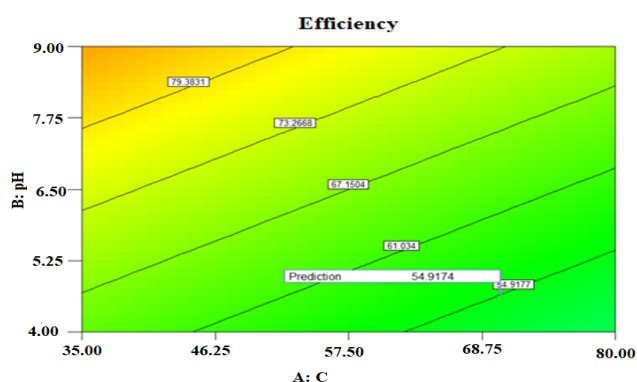
Table 2. The matrix design and the responses

Run	A	B	C	D	E	% Efficiency	q _e
1	35.00	9.00	0.06	35.00	40.00	58.55	1.42
2	80.00	4.00	0.03	85.00	40.00	69.83	23.39
3	35.00	9.00	0.06	85.00	20.00	100	3.45
4	35.00	4.00	0.06	85.00	40.00	90.84	9.71
5	57.50	6.50	0.05	60.00	30.00	48.65	12.54
6	35.00	4.00	0.03	85.00	20.00	69.91	17.06
7	80.00	4.00	0.03	35.00	20.00	42.24	2.28
8	57.50	6.50	0.05	60.00	30.00	50.65	11.42
9	57.50	6.50	0.05	60.00	30.00	49.03	11.59
10	35.00	4.00	0.06	35.00	20.00	68.75	7.18
11	57.50	6.50	0.05	60.00	50.00	79.5	15.9
12	57.50	6.50	0.05	60.00	30.00	55.04	14.27
13	80.00	9.00	0.03	85.00	20.00	29.17	0.98
14	57.50	6.50	0.05	60.00	10.00	34.79	6.99
15	80.00	9.00	0.03	35.00	40.00	100	3.43
16	57.50	6.50	0.05	60.00	30.00	54.8	13.98
17	80.00	4.00	0.06	85.00	20.00	30.7	4.42
18	57.50	6.50	0.05	110.00	30.00	71.06	14.28
19	57.50	1.50	0.05	60.00	30.00	11.45	4.08
20	35.00	4.00	0.03	35.00	40.00	99.13	24.8
21	12.50	6.50	0.05	60.00	30.00	76.11	4.01
22	57.50	11.50	0.05	60.00	30.00	71.36	1.22
23	102.50	6.50	0.05	60.00	30.00	50.98	21.18
24	57.50	6.50	0.08	60.00	30.00	79.51	8.39
25	57.50	6.50	0.05	60.00	30.00	49.25	12.59
26	35.00	9.00	0.03	35.00	20.00	59.74	3.19
27	57.50	6.50	0.01	60.00	30.00	50.19	59.54
28	80.00	9.00	0.06	85.00	40.00	100	1.48
29	57.50	6.50	0.05	10.00	30.00	45.38	9.16
30	35.00	9.00	0.03	85.00	40.00	97.37	5.3
31	80.00	4.00	0.06	35.00	40.00	37.74	5.56
32	80.00	9.00	0.06	35.00	20.00	100	2.14

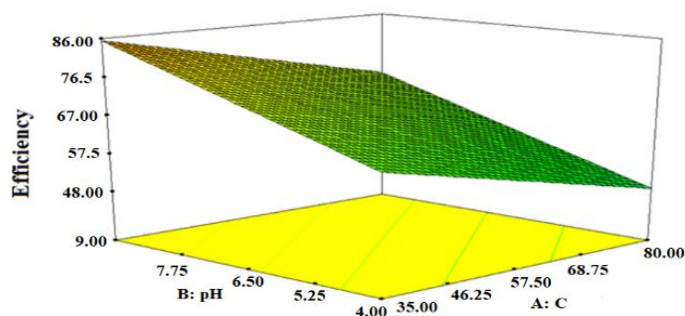
Y is the predicted answer, β_0 is a constant coefficient, $\beta_1, \beta_2, \beta_3$ are linear effects, $\beta_{11}, \beta_{22}, \beta_{33}$ are square effects, $\beta_{12}, \beta_{13}, \beta_{23}$ are interacting effects and ε is the error of prediction equation. One of the most widely used RSM methods is the central composite design (CCD) [42–44]. CCD is basically a two-level factorial method in which central and axial points are added, so that the curvature of the model can be clearly estimated. To optimize the adsorption process and analyze the effects of the independent variables on the response performance (the efficiency of heavy metal removal), the RSM method with CCD design was applied. The effect of the Cd^{2+} concentration (A), pH (B), adsorbent mass (C), contact time (D) and temperature bath (E) on adsorption efficiency was optimized using 5 factors at 5 levels ($-\alpha, -1, 0, +1, +\alpha$) based on CCD in Table 1.

The collected number of 32 experiments containing 6 replicates at the center point was applied to find the mathematical correlate among the independent variable and the corresponding response values. The statistical software Design Expert V.7.1.5 was applied to analyze the experimental data and generate a second-order polynomial model. The optimal conditions for the removal percentage of Cd^{2+} (responses) were determined using the optimal model predict or linear factors equation. Subsequently, analysis of variance (ANOVA) based on the criteria such as P and F values and their comparison with statistical reference value in Table 2 applied for checking adequacy of proposed model and quality of fitting was expressed using value correspond to the coefficient of determination R^2 , adjust and predicted R^2 value.

Design-Expert® Software
 Randomman
 100
 11.45
 X1 = A: C
 X2 = B: pH
 Actual Factors
 C: m = 0.05
 D: time = 60.00
 E: T = 32.53



Design-Expert® Software
 Randomman
 100
 11.45
 X1 = A: C
 X2 = B: pH
 Actual Factors
 C: m = 0.05
 D: time = 60.00
 E: T = 32.53



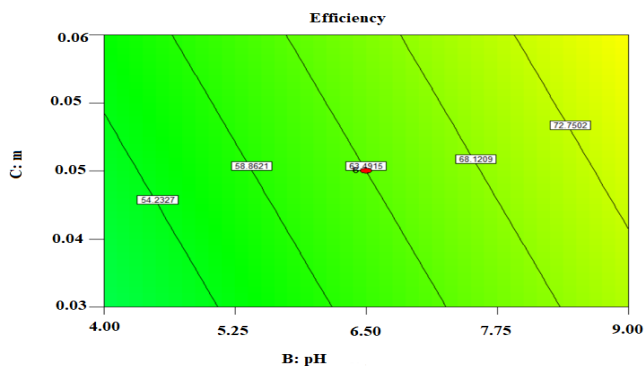
(a)

Design-Expert® Software

Randomman
 ● Design Points
 100
 11.45

X1 = B: pH
 X2 = C: m

Actual Factors
 A: C = 57.50
 D: time = 60.00
 E: T = 30.00

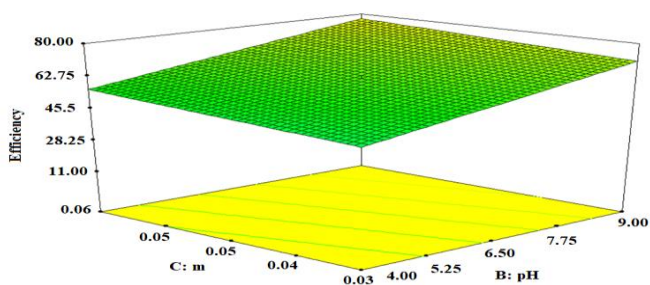


Design-Expert® Software

Randomman
 100
 11.45

X1 = B: pH
 X2 = C: m

Actual Factors
 A: C = 57.50
 D: time = 60.00
 E: T = 30.00



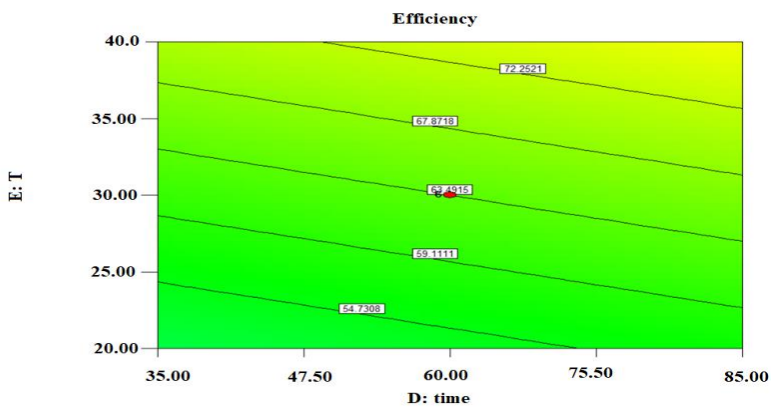
(b)

Design-Expert® Software

Randomman
 ● Design Points
 100
 11.45

X1 = D: time
 X2 = E: T

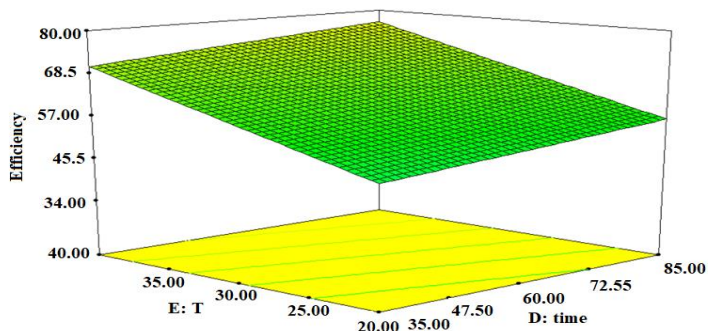
Actual Factors
 A: C = 57.50
 B: pH = 6.50
 C: m = 0.05



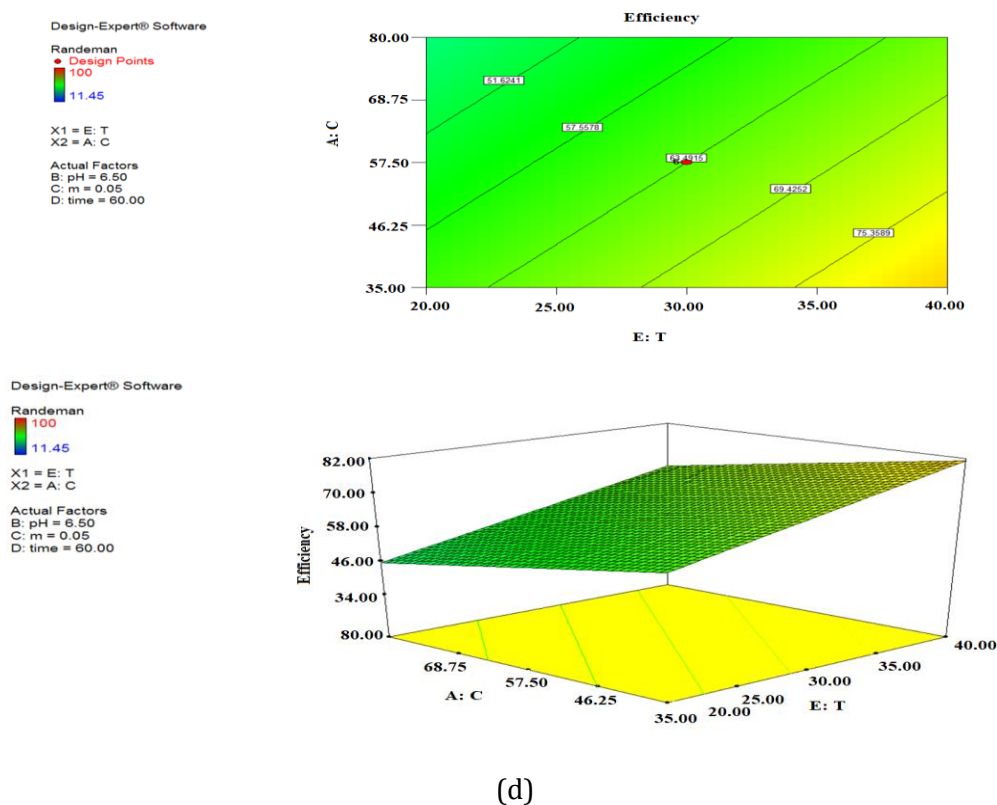
Randomman
 100
 11.45

X1 = D: time
 X2 = E: T

Actual Factors
 A: C = 57.50
 B: pH = 6.50
 C: m = 0.05



(c)



(d)

Figure 1. The 3D surfaces and contour plots for interactive effect variables

Figure 1a-1d reveal the 3D surfaces and contour plots for interactive effect variables.

Result and discussion

Characterization of Adsorbent

XRD was used to determine the constituent phases of the clay minerals, as well as to verify the structural changes after modification. Figure 2 demonstrates the XRD pattern of the $\text{Zn}_2\text{Al-LDH/IC}$. The crystal structures and phase purity of the produced $\text{Zn}_2\text{Al-LDH/IC}$ were examined by XRD. It can be seen that the modification by the indigo carmine caused a reduction in the intensity of the peaks, which may be associated with a possible distortion of the arrangement of the constituent ions of the octahedral and tetrahedral layers [45]. Also, the basal distances did not change,

indicating that the materials maintained their crystallinity.

This result can approve the intercalation of the indigo carmine by the anion exchange in the $\text{Zn}_2\text{Al-LDH}$ compound. The crystallite sizes for the synthesized $\text{Zn}_2\text{Al-LDH/IC}$ were calculated using the Scherer formula (Equation 4).

$$D = \frac{0.9\lambda}{\beta \cos \theta} \quad (4)$$

Where λ is the wavelength of X-ray, β is full width at half maximum of the peak at diffracting angle θ . The calculated crystallite size was 57 nm. The morphology and chemical composition of the synthesized sample were examined using the FE-SEM and EDS. The FE-SEM images of the synthesized sample are revealed in Figure 3. The original sheet and lamellar structure of $\text{Zn}_2\text{Al-LDH}$ changed over intercalation of the indigo carmine.

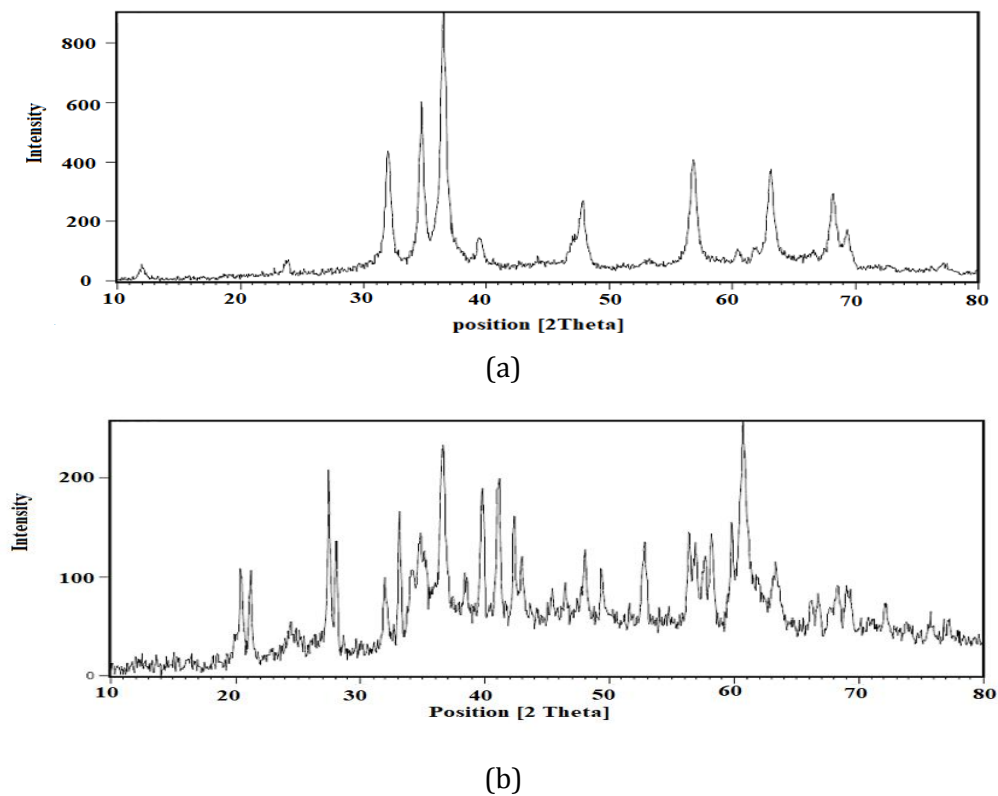


Figure 2. XRD images of (a) Zn₂Al-LDH, (b) Zn₂Al-LDH/IC

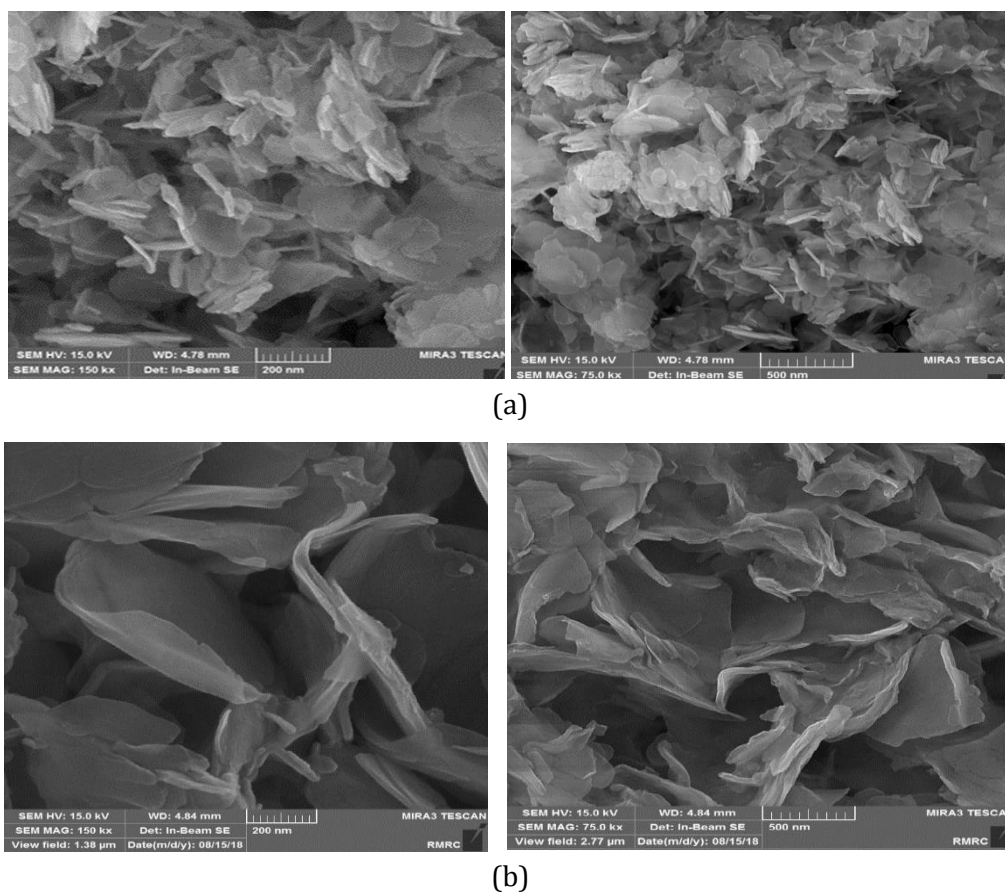


Figure 3. The FE-SEM images of (a) Zn₂Al-LDH and (b) Zn₂Al-LDH/IC

The EDS spectrum of the THE prepared sample (Figure 4) indicates the presence of the relevant elements, demonstrating purity of the synthesized Zn₂Al-LDH/IC.

The adsorption method of the Brunauer, Emmett and Teller (BET) is based on the physical adsorption of a vapour or gas onto the surface of a solid. Such data can be used to analyze the porosity of the materials being studied. In this research study, the BET method was used. The interference by the surrounding phase is especially problematic for the Bruner–Emmet–Teller (BET) N₂ adsorption/desorption isotherm method because the entire surface is modified by vacuum treatment before N₂ adsorption. Figure 5 and Table 3 reveal that the sorbent has an appreciable narrow micro-porosity. The total surface properties of the adsorbent are presented in Table 4.

Design of experiment

Based on the defined experimental conditions in the RSM method and CCD model, 32 different experiments were totally performed according to Table 4 and the results were applied for the determination of optimum conditions of Cd²⁺ removal. The most important variables and their influence

on the response and main interaction with other variables were investigated by analysis of variance (ANOVA) using STATISTICA 10.

The degree of freedom (DF), sum of squared (SS), the contribution of each parameter in the prediction model, the modified root sum squared, the average modified root sum squared, F-value and *p*-values are expressed in the ANOVA tables. In pure statistics, the *p*-value represents the probability value; the probability of the null hypothesis rejection is based on the correctness of this value with respect to the observed data [46]. The *p*-value can also determine the effect of a factor on a response [47]. Lower *p*-values correspond to higher importance of the model and the factor. *p*-values lower than 0.05 indicate that the parameter under study is important in the results obtained from the model [48]. In ANOVA, the *F*-value is the ratio of the mean regression sum of squares divided by the mean error sum of squares. The higher the *F*-value for an answer is, the more important is the effects of the considered levels of factors [49]. According to the *F*-values and *p*-values, the pH, metal ion concentration (Con) and adsorbent dosage (Dose), time and temperature bath are the main parameters (Table 4 and Table 5).

Figure 4. The EDS image of Zn₂Al-LDH/IC

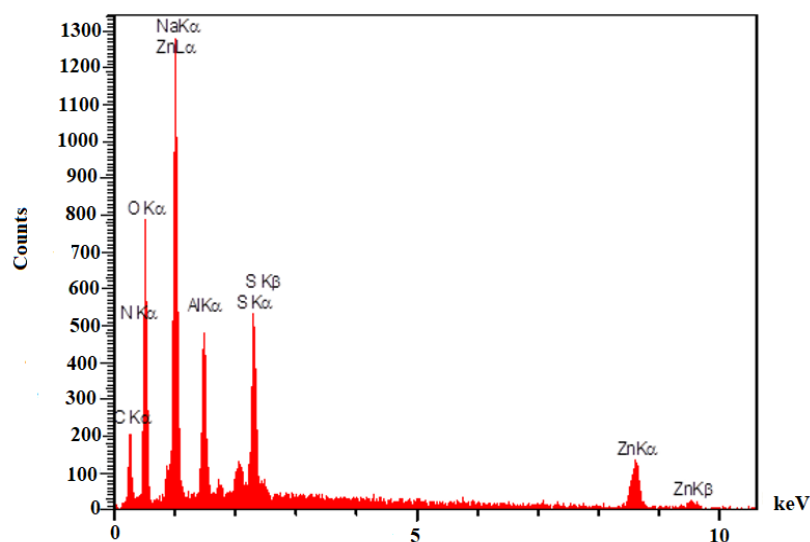


Figure 5. The BET image of Zn₂Al-LDH/IC

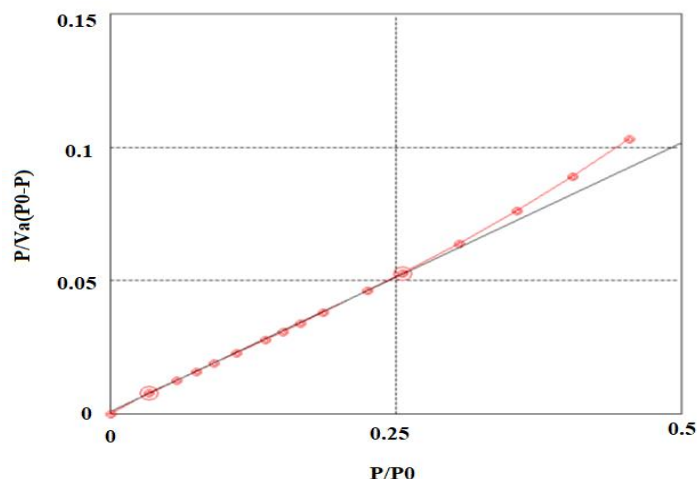


Table 3. Surface area and porosity measurement (BET Method) of Zn₂Al-LDH/IC

Sample	Surface Area (m ² /g)	Micropore Vol. (cc/g)	Micropore Size (nm)
Zn ₂ Al-LDH/IC	21.516	0.1942	36.099

Table 4. The results of ANOVA for the response 1, %fficiency and surface linear model

Source	Sum of Squares	DF	Mean Square	F Value	p-value Prob > F	
Model	7066.06	5	1413.21	3.38	0.0175	significant
A-C	1424.00	1	1424.00	3.40	0.0764	
B-pH	2720.23	1	2720.23	6.50	0.0170	
C-m	252.24	1	252.24	0.60	0.4444	
D-time	222.19	1	222.19	0.53	0.4726	
E-T	2447.40	1	2447.40	5.85	0.0229	
Residual	10875.12	26	418.27			
Lack of Fit	10832.15	21	515.82	60.02	0.0001	significant
Pure Error	42.97	5	8.59			
Cor Total	17941.18	31				

DF: degrees of freedom

SS: sums of squares, the sum of the squared differences between the average values and the overall mean

Ms: mean squares, the sum of squares divided by df

SD: standard deviation

R²: R-Squared (coefficient of determination)

F-value: test for comparing term variance with residual (error) variance

Prob>F: the probability of seeing the observed F value if the null hypothesis is true

Residual: consists of terms used to estimate the experimental error

Lack of fit: variation of the data around the fitted model

Pure error: variation in the response in replicated design points

Cor total: totals of all information corrected for the mean

Table 5. Optimization Point of Zn₂Al-LDH/IC

C*	pH*	m*	time*	T*	Desirability	
52	4.13	0.06	36	309.65	1.000	Selected

Moreover, the most effective parameters were determined based on the p- and F-values. The below empirical relationship (Equation 5) between the response and independent variables as the Linear equation is applicable to predict real behavior of the adsorption system at the various conditions.

$$\% \text{ Efficiency} = +9.86464 - 0.34235 * C + 4.25850 * \text{pH} + 176.19085 * m + 0.12171 * \text{time} + 1.00983 * T \quad (5)$$

Generally, when the coefficient of each parameter is increased, it confirms a highly positive influence on the response. The negative value of each parameter shows that, there is a reverse correlation between the responses and the parameter, indicating that the negative value results in the achievement of maximum responses. According to the Equation 5, the pH, amount of adsorbent, time and temperature bath have a positive effect and concentration of Cd²⁺ have a negative effect on yield process (removal percentage of Cd²⁺). As seen in Equation 5, the factor of pH, amount of adsorbent, time and temperature bath have the most positive effect on the removal percentage of Cd²⁺. It means that with increasing of the adsorbent dosage, the removal of the Cd²⁺ increased.

Optimization of adsorption conditions

Response surface methodology (RSM) combination with CCD was used to optimize the critical factors and describe the nature of the response surface in the experiment. Figure 1 represents the relevant fitted response surfaces for the design and depicts the response surface plots of removal percent versus significant variables. These plots were obtained for a given pair of factors at center values of other variables. The curvatures of plots indicate the interaction between the

variables. The Cd²⁺ removal percentage greatly has positive relation with mixing. The rapid and fast transfers of Cd²⁺ molecules to the adsorbent surface that admit rapid equilibrium, confirm the suitability and efficiency of mixing with magnetic stirrer as powerful toll for wastewater treatment. The results demonstrated that, the initial adsorption rate is very rapid because of high available surface area and vacant site of adsorbent that enhance the interface and driving force. The interaction of adsorbent dosage with other variables (Figure 1b) showed a significant trend between Cd²⁺ removal percentages with adsorbent dosage. At lower amount of adsorbent, the removal percentage because of high ratio of Cd²⁺ molecule to vacant site significantly decreased. Figure 1a and 1b presents the interaction of pH with initial Cd²⁺ concentration and adsorption dosage, respectively. The Zn₂AL-LDH/IC removal percentage gradually enhance by rising the pH. This result is attributed to the fact that at low pH due to protonation of H₂O, the adsorbent surfaces get positive charge. Therefore, strong repulsive forces between the cationic Cd²⁺ molecules and adsorbent reduced the Cd²⁺ removal percentage. However, at the pH values above 6, the Cd²⁺ ions precipitated as hydroxide in aqueous solution. Therefore, the increase in the initial pH leads to less decrease in the Cd²⁺ removal percentage. Figure 1a and 1c demonstrate the effect of initial Cd²⁺ concentration and its interaction with other factors. It was found that, in despite of the increase in the amount of Cd²⁺ concentration, its removal efficiency was decreased and at lower Cd²⁺ concentrations, the ratio of solute concentrations to adsorbent sites is lower, which cause an increase in Cd²⁺ removal. At the higher concentrations, lower adsorption yield is due to the saturation of adsorption sites. On the other hand, the percentage removal of the Cd²⁺ was higher at the medium

initial Cd^{2+} concentrations and smaller at higher initial concentrations, which clearly indicating that the adsorption of Cd^{2+} from its aqueous solution was dependent on its initial concentration. The profile for the predicted values and desirability option in the STATISTICA 7.0 software was used to optimize the variable influences (Figure 1). Profiling the desirability of responses involves specifying the DF for each dependent variable (removal %) by assigning predicted values. The CCD design matrix results (Table 1) show the maximum (59.54%) and minimum (0.98%) for Cd^{2+} removal percentage. The individual desirability scores were used to calculate the removal percentage and the desirability of 1.0 was selected as the target value (Table 4). The basis of these calculations and desirability score of 1.0 was obtained at the optimum conditions (Table 5) of 36 min for time, 0.06 g of adsorbent at pH 4.13 and initial Cd^{2+} concentration of 52 mg/L^{-1} . The triplicate conduction of similar experiments at optimized value of all parameters has RSD% lower than 3% and are closely correlated with the data obtained from desirability optimization analysis using CCD.

Analysis of ANOVA data

The linear model was suggested by the software for yield. ANOVA data (Table 6) demonstrates the Model F-value of 3.38, implying that the model is significant and only a 1.75% chance that a "Model F-Value" can lead to the large value that can be caused by noise. Values of "Prob>F" less than 0.0500 indicated that, the model terms are significant.

In this case B, E are significant model terms. Values greater than 0.1000 indicate that, the model terms are not significant. If there are many insignificant model terms (not counting those required to support hierarchy), model reduction may improve your model. The "Lack of Fit F-value" of 60.02 implies the Lack of Fit is significant. There is only a 0.01% chance that a "Lack of Fit F-value" this large could occur due to noise. Significant lack of fit is bad we want the model to fit. Table 6 demonstrates the chosen amounts for the equilibrium isotherms models, adsorption kinetics, and thermodynamic study in base of optimum condition.

Equilibrium isotherms models

The equilibrium adsorption isotherm was used to give useful information about the mechanism, properties and tendency of adsorbent to ward each dye molecule. In general, an isotherm of the adsorption describes the phenomenon governed by the retention or mobility of a substance in solid phase at constant temperature. The experimental data was fitted to the models of Langmuir, Freundlich and Tempkin. According to our previous study [50], and based on their linear form, slopes and intercepts, respective constants are evaluated (Table 7). Also, the experimental results based on the higher values of correlation coefficients ($R^2 \sim 1$) demonstrated reasonable applicability of Langmuir and Freundlich models for the Cd^{2+} adsorption onto $\text{Zn}_2\text{Al-LDH/IC}$.

Table 6. Experimental factors for isotherm, kinetic, and thermodynamic studies

Factors	Unit	Type of study	levels						
Concentration(C)	mg/L	isotherm	22	32	42	52*	62	72	82
pH			4.13	4.13	4.13	4.13*	4.13	4.13	4.13
adsorbent dosage(m)	g		0.06	0.06	0.06	0.06*	0.06	0.06	0.06
Contact time(time)	min	kinetic	21	26	31	36*	41	46	51
Temperature(T)	°C	thermodynamic	21.5	26.5	31.5	36.5*	41.5	46.5	51.5

*: optimum point

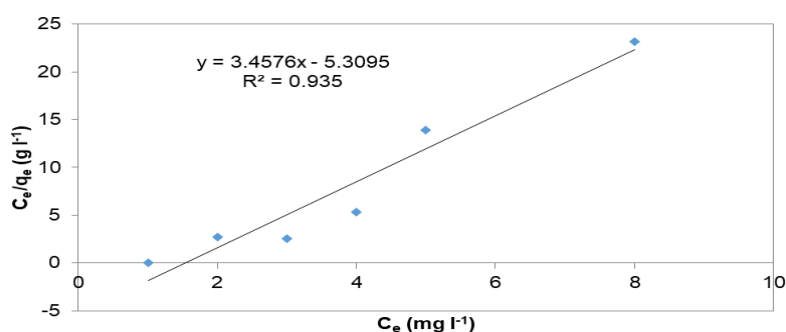
The experimental results from the adsorption of Cd^{2+} by $\text{Zn}_2\text{Al-LDH/IC}$ were analyzed using the Langmuir, Freundlich, and Temkin models. The Langmuir isotherm can be considered as Equation 6.

$$C_e/q_e = 1/q_{\max} K_L + C_e/q_{\max} \quad (6)$$

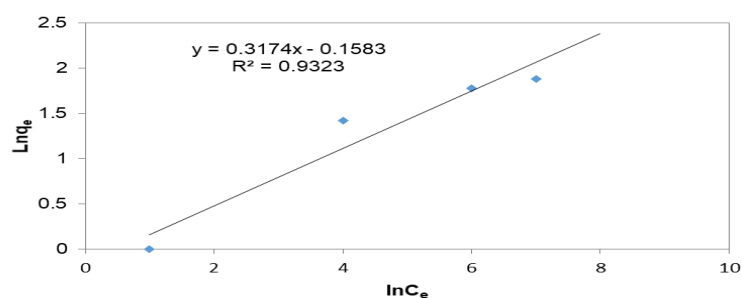
Where C_e (mg/L^{-1}) is the concentration at equilibrium, q_e (mg/g^{-1}) is amount of adsorbate adsorbed per gram of adsorbent at equilibrium, K_L (the Langmuir constants associated with energy of adsorption, (L/mg), the q_m (mg/g^{-1}) is the maximum adsorption

capacity of the adsorbent corresponding to monolayer formation and illustrates the maximum value of q_e that can be achieved when C_e is increased. Figure 6-a shows the linear plot of C_e/q_e vs. C_e of Langmuir isotherm. The values of q_m and K_L were determined from slope and intercepts of the plots and are presented in Table 8. The Freundlich's adsorption isotherm model can be applied for a multilayer heterogeneous adsorption and expressed as Equation 7 [51]:

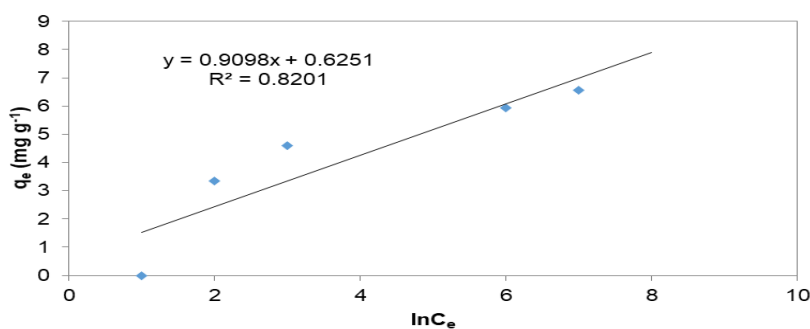
$$\log q_e = 1/n \log C_e + \log K_F \quad (7)$$



(a)



(b)



(c)

Figure 6. The plots of (a) Langmuir equilibrium isotherm, (b) Freundlich isotherm, and (c) Temkin isotherms

Where K_F (l/g^{-1}) is the Freundlich isotherm constants related to the maximum adsorption capacity and n is the intensity of adsorption. Figure 6b shows the linear plot of $(\ln q_e \text{ vs. } \ln C_e)$ of Freundlich isotherm. The plot of $\ln q_e \text{ vs. } \ln C_e$ was employed to generate the intercept value of K_F and the slope of $1/n$ (Table 8). The heat of the adsorption and the interaction of adsorbent adsorbate were studied using Temkin isotherm model as expressed in Eq. (8) [52]:

$$q_e = B_T \ln K_T + B_T \ln C_e \quad (8)$$

In this model, B_T is the Temkin constant related to the heat of adsorption (J/mol^{-1}), T is the absolute temperature (K), and K_T is the equilibrium binding constant (L/mg^{-1}). Figure 6c shows the linear plot of $q_e \text{ vs. } \ln C_e$ of Temkin isotherm model. The constant parameters of isotherm equations and the correlation coefficient (R^2) for isotherm models are summarized in Table 7. The high correlation coefficient at different conditions represents the applicability of Langmuir model for investigation of the experimental data.

Adsorption kinetics

To control the mechanisms of the adsorption processes such as mass transfer and chemical reactions, different

kinetic models used sorption reactions and, the rate of adsorption (which is one of the criteria for efficiency of adsorbent) and the mechanism of adsorption can be concluded from this studies [53, 54]. Adsorption kinetics of Cd^{2+} was evaluated using four models such as pseudo-first-order, pseudo-second order, intra particle diffusion, and Elovich models (39 Lin Deng). The various parameters were calculated from the plots of the kinetic model equations (Table 8). All the kinetic equations are shown in Table 8, where k_1 and k_2 ($g/mg^{-1}/min^{-1}$) are the pseudo-first-order and pseudo-second-order rate constants for adsorption. R^2 is the correlation coefficient to express the uniformity between the model-predicted values and the experimental data. α ($mg/g^{-1}/min^{-2}$) is the initial adsorption rate. β ($g/mg^{-1}/min^{-1}$) is the desorption constant related to the extent of surface coverage and activation energy for chemisorption. All of the investigated models were fitted by a linear regression to the experimental data, evaluating their appropriateness based on the corresponding correlation coefficients R^2 . The correlation coefficient (R^2) and agreement between the experimental and calculated values of q_e , are the criteria for the applicability of each models.

Table 7. Isotherm constant parameters and correlation coefficients calculated for the adsorption of Cd^{2+} onto $Zn_2Al-LDH/IC$

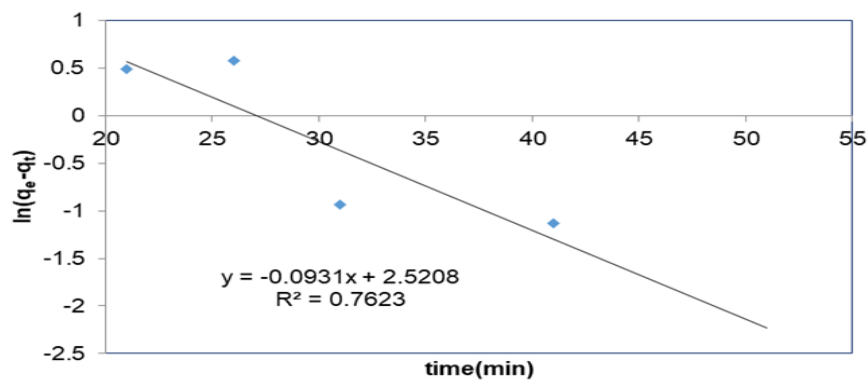
Isotherm	Parameters	Value
Langmuir	q_m (mg/g^{-1})	0.2892
	K_L (L/mg^{-1})	-0.6542
	R^2	0.9350
	n	3.1506
Freundlich	K_F (L/mg^{-1})	0.8536
	R^2	0.9323
Temkin	B_T	0.9098
	K_T (L/mg^{-1})	1.9897
	R^2	0.8201

Good agreement between two q_e values and the high values of ($R^2 \sim 1$) indicated that the adsorption system under study follows the pseudo-first order kinetic model (Table 8). A pseudo-first order adsorption mechanism assumes the rate of occupying adsorption sites is proportional to the square of the number of unoccupied sites. The equation of this model is shown in Equation 9.

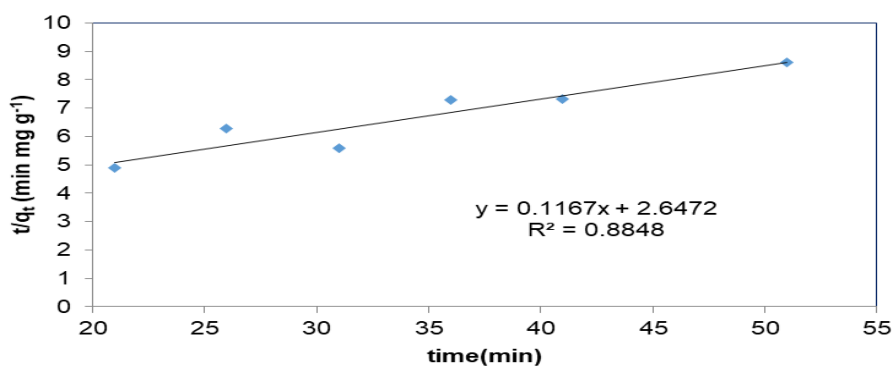
$$\ln(q_e - q_t) = \ln q_e - K_1 t \quad (9)$$

Where q_e is the equilibrium adsorption capacity (mg/g^{-1}) for the pseudo-first-order the adsorption, q_t is the adsorption capacity at time t (mg/g^{-1}) and k_1 (min^{-1}) is the rate constant of the pseudo-first-order adsorption. The values of q_e and k_1 obtained from the slope and intercept of $\ln(q_e - q_t)$ versus t . According to the assumptions of this model, adsorption process involves different mechanisms including chemical and electrostatic interactions between functional groups on the surface of adsorbent and adsorbate molecules. The linear regressions and kinetic parameters are listed in Figure 7 and Table 8, respectively. It is clear that correlation coefficients for the pseudo-first-order model ($R^2 \sim 0.97$) are higher than that for the pseudo-second-order model ($R^2=0.915$), indicating that the present system can be well defined by the pseudo-first-order kinetic model in the adsorption step. Additionally, the theoretical equilibrium sorption capacity ($q_{e,\text{cal}}$) calculated by the pseudo-first-order model at all concentrations are also in good agreement with those obtained from experiments ($q_{e,\text{exp}}$). The fitness of the pseudo-first-order kinetic model reveals that the rate-limiting step in adsorption is controlled by chemical process [55]. The Elovich equation is the integration of the rate equation with the same boundary conditions as the pseudo-first-order equation, which is used to interpret the predominantly chemical adsorption on highly heterogeneous

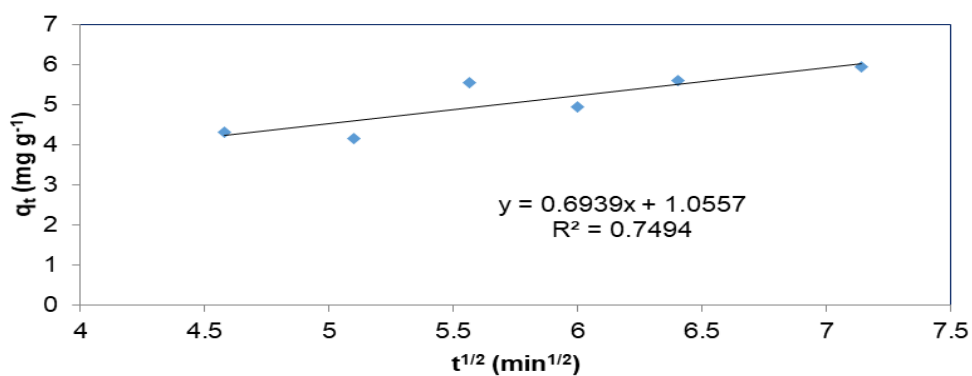
adsorbents [56]. As depicted in Figure 7d, the plots of q_t versus $\ln(t)$ display relative good linear correlation, suggesting that the Elovich equation is able to describe the adsorption kinetic and ion exchange is involved in the system. Due to the mesoporous structure of the adsorbent, diffusion is also expected to influence the adsorption rate. The plots of q_t versus $t^{1/2}$ at different initial Cd^{2+} concentrations are illustrated in Figure 7c. All the three plots exhibited multi-straight-line nature, indicating that more than one process affects the adsorption. The first rapid stage is attributed to mass transfer across the external boundary layer film to the outer surface of adsorbent particles (film diffusion) [57], the second linear portion refers to the pore diffusion that Cd^{2+} move within the micro-, meso- and macro-pores of adsorbent particles (pore diffusion), and the third stage with the lowest slope is ascribed to surface diffusion mechanism at a site on the adsorbent surface (physical/chemical reaction or surface diffusion) [58]. The fitting results implied that, the intra-particle diffusion of Cd^{2+} to an adsorption site on the particle surface is the rate limiting step in the adsorption process. All the intra-particle diffusion rate constants C related to the boundary layer thickness in this study are not zero, revealing that the adsorption process may not be mainly controlled by intra-particle diffusion [59]. The kinetic analysis based on the kinetic models including pseudo first- and second-order, Elovich and intraparticle diffusion (Figure 7a-d) give good knowledge about the rate and mechanism of adsorption. From all the correlation coefficients and above analysis, it can be concluded that the pseudo-second-order kinetic model is the most suitable model for adsorption of Cd^{2+} onto $\text{Zn}_2\text{Al-LDH/IC}$. Table 8 summarizes the obtained results of each model. The highest R^2 value of this model (1.0000) confirmed the applicability of this model to interpret the experimental data.



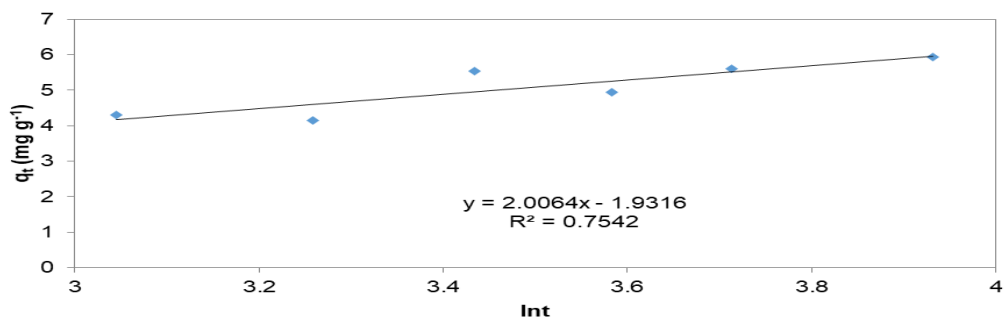
(a)



(b)



(c)



(d)

Figure 7. The plot of (a) pseudo- first- order, (b) pseudo -second-order, (c) intra particle diffusion (d) Elovich

Table 8. Kinetic parameters for removal Cd²⁺ onto Zn₂Al-LDH/IC

Model	Equation	Plot	Parameters	Value
Pseudo-first-order	$\log(q_e - q_t) = \log(q_e) - \frac{k_1 t}{2.303}$	ln (q _e - q _t) vs. t	K ₁ (min ⁻¹)	-0.0931
			q _e	12.4385
			R ²	0.7623
Pseudo-second-order	$\frac{t}{q_t} = \frac{1}{k_2 q_e^2} + \left(\frac{1}{q_e}\right) t$	t/q _t vs. t	k ₂ (g mg ⁻¹ /min ⁻¹)	60.0486
			q _e	0.3778
			R ²	0.8848
Intra particle diffusion	q _t = K _{id} t ^{1/2} + C	q _t vs. t ^{1/2}	K _{id}	0.6939
			C	1.0557
			R ²	0.7494
Elovich	q _t = 1/β ln(αβ) + 1/β ln(t)	qt vs. ln(t)	α	0.7662
			β	0.4984
			R ²	0.7542

Thermodynamic study

To study the thermodynamic aspects of Cd²⁺ adsorption on adsorbent, the thermodynamic parameters including enthalpy change (ΔH°), entropy change (ΔS°) and the change in Gibbs free energy (ΔG°) were calculated [55]. Thermodynamic parameters play an essential role in the adsorption process and provide important information about adsorption mechanism and its spontaneous or non-spontaneous behavior. The Gibbs free energy (ΔG°), enthalpy change (ΔH°), and entropy changes (ΔS°) for the adsorption system were obtained using the Equations 10 and 11.

$$\Delta G^\circ = \Delta H^\circ - T\Delta S^\circ \quad (10)$$

$$\Delta G^\circ = -RT \ln K_C \quad (11)$$

Where K_c (mL/g⁻¹) is the solid-liquid distribution coefficient that can be obtained by the intercept of plot of ln (q_e/C_e) vs. q_e, (Figure 8a), R is the universal gas constant (8.314 J/mol·K⁻¹) and T is the absolute temperature.

$$\ln K_C = \frac{\Delta S^\circ}{R} - \frac{\Delta H^\circ}{RT} \quad (12)$$

The plots of ln K_c vs. 1/T give the straight line from which ΔH° and ΔS° are

calculated from the slope and intercept, respectively (Figure 8b).

The obtained ΔG°, ΔH° and ΔS° are summarized in Table 9. The negative value of ΔG° (-251.6 J/mol⁻¹), indicating that the spontaneity of the process and the great affinity of Cd²⁺ for the adsorbent used. The positive ΔH° values indicate that the process is endothermic and chemical in nature. The increase in adsorption with temperature is associated with the raising of the diffusion rate of molecules of adsorbate with a higher quantity of molecules with sufficient energy to undergo interaction with active surface sites [60]. The positive value of ΔS° indicated an increase in the disorder of the adsorbed species, possibly along with the changes in the configuration of the adsorbate molecules and the surface of the adsorbent compounds.

The negative value of the ΔG° (-251.6 J/mol⁻¹) indicated that the feasible and spontaneous nature of the adsorption. The negative value of the ΔH° (-2.2207 J/mol⁻¹) suggested that the adsorption process was endothermic. The positive value of the ΔS° (0.8281 J/mol⁻¹/K⁻¹) also suggested increased random at the solid-solution interface during the fixation of Cd²⁺ on the active sites of the adsorbent.

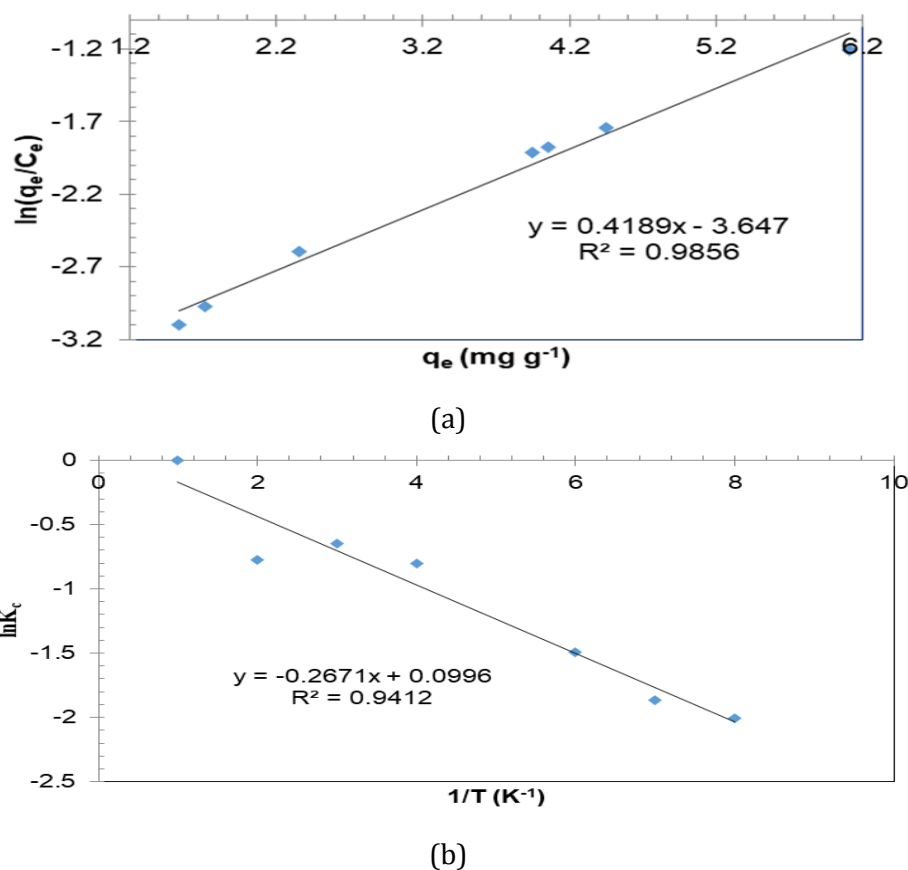


Figure 8. The Van't Hoff plots of Zn₂Al-LDH/IC adsorption to determine (a) ΔH° and ΔS° (b) ΔG°

Table 9. Thermodynamic parameters for adsorption of Cd²⁺ by Zn₂Al-LDH/IC

Parameters	ΔH° (J mol ⁻¹)	ΔS° (J mol ⁻¹ K ⁻¹)	ΔG° (J mol ⁻¹)	T, K	ln K _C	R ²
Zn ₂ Al-LDH/IC	2.2207	0.8281	-238.5	290.65	0.0987	0.9412
			-242.6	295.65		
			-246.76	300.65		
			-250.9	305.65		
			-255.0	310.65		
			-259.2	315.65		
			-263.3	320.65		

Reusability of Zn₂Al-LDH/IC

One of the steps of examination of the economic viability of the adsorption process consisted of reusing the adsorbents in several successive separation processes. The percentage removal of the Cd²⁺ using the adsorbent in five cycles of adsorption is

shown in Figure 9. After the 5th use, the percentage of the Cd²⁺ adsorbed decreased 98%, 97.4%, 96.3%, 95.8%, and 94.8%, respectively. So, the obtained results revealed that, the Zn₂Al-LDH/IC can be reused for five times without any reduction in their efficiency (Figure 9).

Determination of zero point charge

Determination of point of zero charge (pHz) was done to determine the surface charge (or the stability) of Zn₂Al-LDH/IC. For determination of pHz, a solution of 0.1 M NaCl was prepared, and its initial pH was adjusted between 4.0 and 11.0 using HCl and NaOH solutions. Then, 20 mL of 0.1 M

NaCl solution was taken in 25 mL flasks and 0.015 g of Zn₂Al-LDH/IC was added to each solution. These flasks were kept for 24 h and the final pH of the solutions was measured with a pH meter. Graphs were plotted between final pH and initial pH. As seen in Figure 10, at pH of 7.35 and Δ pH of 0, the pHz was found to be 7.35.

Figure. 9 The ability of reusing Zn₂Al-LDH/IC in five successive separation processes

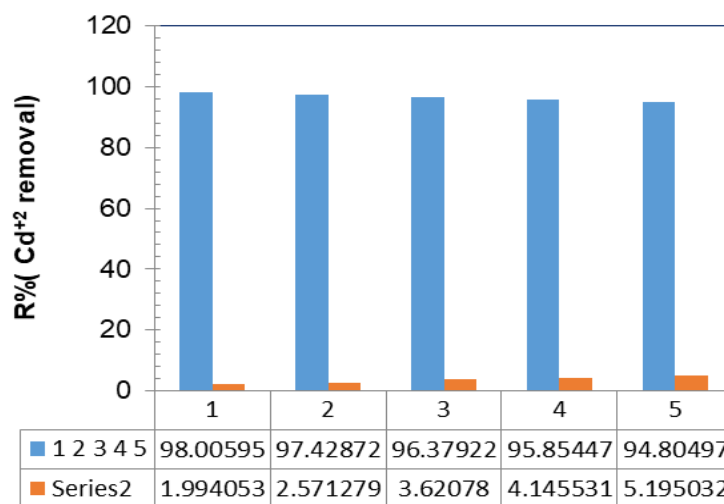
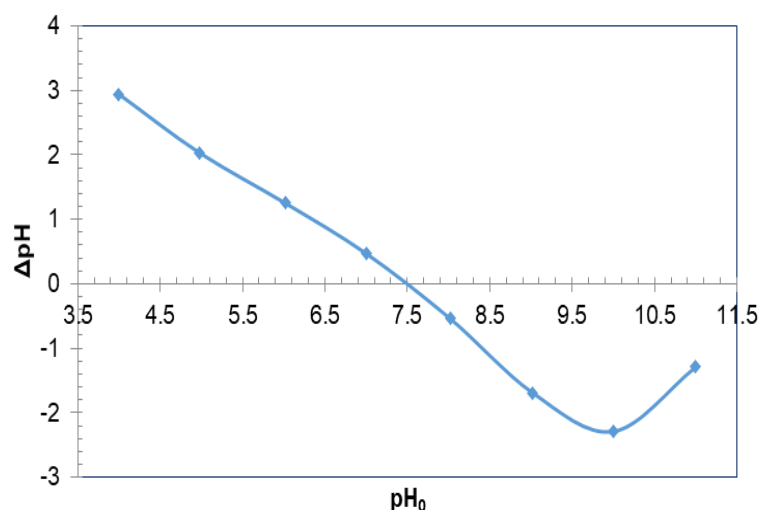


Figure 10. The Zero point charge determination



Conclusions

The goal of this work was to use response surface modeling centered on five variables of central composite design for determining the individual as well as the combined effect of several parameters such as initial

concentration of Cd²⁺, pH, adsorbent dosage, temperature, and contact time. The regression analysis and optimization of variables were carried out using the design expert software for predicting the response in all experimental sections. The experimental values were found to be in well agreement

with the expected values from the model. The optimum conditions were found to be initial Cd²⁺ concentration of 52 mg/L, a pH value of 4.13, adsorbent dosage of 0.06 g, the temperature of 309.7 K, and contact time of 36 min.

Acknowledgement

The financial support of the research council of Payame Noor University of Isfahan is gratefully acknowledged.

Disclosure statement

No potential conflict of interest was reported by the authors.

References

- [1] M. Farasati, S. Haghighi, S. Boroun, *Desalin. Water Treat.*, **2016**, *57*, 11162–11172.
- [2] J. Sheng, W. Qiu, B. Xu, H. Xu, C. Tang, *Environ. Sci. Pollut. Res.*, **2016**, *23*, 11034–11045.
- [3] P. Dey, D. Gola, A. Mishra, A. Malik, D.K. Singh, N. Patel, M. Von Bergen, N. Jehmlich, *J. Hazard. Mater.*, **2016**, *318*, 679–685.
- [4] WHO, *Guidelines for the safe use of wastewater, excreta and greywater*, World Health organization. **2006**; Vol. I, p. 95.
- [5] G.F. Nordberg, K. Nogawa, M. Nordberg, *Cadmium, Handbook on the Toxicology of Metals*, fourth edition, **2014**, p. 667.
- [6] G. Mohammadnezhad, M. Dinari, R. Soltani, *New J. Chem.*, **2016**, *40*, 3612–3621.
- [7] H. Cui, Y. Fan, J. Yang, L. Xu, J. Zhou, Z. Zhu, *Chemosphere*, **2016**, *161*, 233–241.
- [8] M. Dinari, R. Soltani, G. Mohammadnezhad, *J. Chem. Eng. Data.*, **2017**, *62*, 2316–2329.
- [9] C.G. Lee, J.A. Park, J.W. Choi, S.O. Ko, S.H. Lee, *Water Air Soil Pollut.*, **2016**, *227*, 456–463.
- [10] M. Li, M. Y. Gong, A. Lyu, Y. Liu, H. Zhang, *Appl. Surf. Sci.*, **2016**, *383*, 133–141.
- [11] G. Mohammadnezhad, S. Abad, R. Soltani, M. Dinari, *Ultrason. Sonochem.*, **2017**, *39*, 765–773.
- [12] K. Yang, L.G. Yan, Y.M. Yang, S.J. Yu, R.R. Shan, H.Q.; Yu, B.C. Zhu, B. Du, *Sep. Purif. Technol.*, **2014**, *124*, 36–42.
- [13] F. Ahmadi, H. Esmaeili, *Desalin water treat.*, **2018**, *110*, 154–167.
- [14] R. Foroutan, R. Mohammadi, S. Farjadfard, H. Esmaeili, M. Saberi, S. Sahebi, S. Dobaradaran, B. Ramavandi, *Environ. Sci. Pollut. Res. Int.*, **2019**, *26*, 6336–6347.
- [15] I. Khoshkerdar, H. Esmaeili, *Acta Chim. Slovenica.*, **2019**, *66*, 208–216.
- [16] F. Foroutana, H. Esmaeilib, A.M. Sanatic, M. Ahmadid, B. Ramavandif, *Desalin water treat.*, **2018**, *135*, 236–246.
- [17] J. Das, D. Das, K.M. Parida, *J. Coll. Interface Sci.*, **2006**, *301*, 569–574.
- [18] X. Cai, X. Shen, L. Ma, Z. Ji, C. Xu, A. Yuan, *Chem. Eng. J.*, **2015**, *268*, 251–259.
- [19] S. Nishimura, A. Takagaki, K. Ebitani, *Green Chem.*, **2013**, *15*, 2026–2042.
- [20] C. Li, M. Wei, D.G. Evans, X. Duan, *Small*, **2014**, *10*, 4469–4486.
- [21] K. Ladewig, Z.P. Xu, G.Q. Lu, *Exp. Opin. Drug. Deliv.*, **2009**, *6*, 907–922.
- [22] M.H. Kim, D.H. Park, J.H. Yang, Y.B. Choy, J.H. Choy, *Int. J. Pharm.*, **2013**, *444*, 120–127.
- [23] J. Das, B.S. Patra, N. Baliarsingh, K.M. Parida, *Appl. Clay. Sci.*, **2006**, *32*, 252–260.
- [24] K.H. Goh, T.T. Lim, Z. Dong, *Water. Res.*, **2008**, *42*, 1343–1368.
- [25] D. Bharali, R.C. Deka, *Coll. Surfaces A.*, **2017**, *525*, 64–76.
- [26] K. Abdellaoui, I. Pavlovic, M. Bouhent, A. Benhamou, C. Barriga, *Appl. Clay. Sci.*, **2017**, *143*, 142–150.
- [27] R.M. Dos Santos, R.G. Gonçalves, V.R. Constantino, C.V. Santilli, P.D. Borges, J. Tronto, F.G. Pinto, *Appl. Clay. Sci.*, **2017**, *140*, 132–139.
- [28] W. Yao, S. Yu, J. Wang, Y. Zou, S. Lu, Y. Ai, N.S. Alharbi, A. Alsaedi, T. Hayat, X. Wang, *Chem. Eng. J.*, **2017**, *307*, 476–486.
- [29] C.M. Becker, A.D. Gabbardo, F. Wypych, S.C. Amico, *Compos Part A Appl. Sci. Manuf.*, **2011**, *42*, 196–202.

- [30] Z. Gu, J.J. Atherton, Z.P. Xu, *Chem. Commun.*, **2015**, 51, 3024–3036.
- [31] M.I. Carretero, *Appl. Clay Sci.*, **2002**, 21, 155–163.
- [32] M.R. Pérez, I. Pavlovic, C. Barriga, J. Cornejo, M.C. Hermosín, M.A. Ulibarri, *Appl. Clay Sci.*, **2006**, 32, 245–251.
- [33] S. Yanming, L. Dongbin, F. Lihui, C. Shuai, Md. Haque, *Arab. J. Chem.* **2017**, 10, S2295–S2301.
- [34] I. Pavlovic, M.R. Pérez, C. Barriga, M.A. Ulibarri, *Appl. Clay Sci.*, **2009**, 43, 125–129.
- [35] S. Chatterjee, A. Kumar, S. Basu, S. Dutta, *Chem. Eng. J.*, **2012**, 181–182, 289–299.
- [36] L. Deng, Si. Zhou, Li. Wang, Sh. Zhou, *J. Phys. Chem. Solid.*, **2017**, 104, 79–90.
- [37] J. Mousavi, M. Parvini, *Int. J. Hydrogen Energy.*, **2016**, 41, 5188–5201.
- [38] S. Chatterjee, A. Kumar, S. Basu, S. Dutta, *Chem. Eng. J.*, **2012**, 181, 289–299.
- [39] M. Amini, H. Younesi, N. Bahramifar, *Chemosphere.*, **2009**, 75, 1483–1491.
- [40] M. Vaezi, M.B. Vishlaghi, M.F. Tabriz, O.M. Moradi, *J. Alloys Compd.*, **2015**, 635, 118–123.
- [41] N. Marchitan, C. Cojocar, A. Mereuta, G. Duca, I. Cretescu, M. Gonta, *Sep. Purif. Technol.*, **2010**, 75, 273–285.
- [42] M.S. Bhatti, A.S. Reddy, R.K. Kalia, A.K. Thukral, *Desalination.*, **2011**, 269, 157–162.
- [43] S. Bajpai, *J. Hazard Mater.*, **2012**, 227, 436–444.
- [44] M. Sarkar, P. Majumdar, *Chem. Eng. J.*, **2011**, 175, 376–387.
- [45] A.K. Panda, B.G. Mishra, R.K. Singh, *Coll. Surf. A.*, **2010**, 363, 98–104.
- [46] G. Mazerolles, D. Mathieu, R. Phan-tan-luu, A. M. Siouffi, *J. Chromatogr. A*, **1989**, 485, 433–451.
- [47] M.S. Kumar, B. Phanikumar, *Environ. Sci. Pollut. Res.*, **2013**, 20, 1327–1343.
- [48] D.C. Montgomery, *Design and analysis of experiments.*, John Wiley & Sons, **2017**.
- [49] R.H. Myers, D. C. Montgomery, C.M. Anderson-Cook, *Response surface methodology: process and product optimization using designed experiments.*, John Wiley & Sons, **2016**.
- [50] N. Samadani Langeroodi, Zh. Farhadraresh, A. Dehno Khalaj. *Green Chem. Lett. Rev.*, **2018**, 11, 404–413.
- [51] D. Citak, M. Tuzen, M. Soylak, *Food Chem. Toxicol.*, **2009**, 47, 9, 2302–2307.
- [52] K.A.H. Said, N.Z. Ismail, R.L. Jama'in, N.A.M. Alipah, N.M. Sutan, G. G. Gadung, R. Baini, N.S.A. Zauzi, *Int. J. Eng. Technol.*, **2018**, 7, 91–93.
- [53] E. Koohzad, D. Jafari, H. Esmaeili, *Chem Select.*, **2019**, 4, 12356–12367.
- [54] R. Foroutan, R. Mohammadi, S. Farjadfard, H. Esmaeili, B. Ramavandi, G.A. Sorial, *Adv. Powder Technol.*, **2019**, 30, 2188–2199.
- [55] B.K. Nandi, A. Goswami, M.K. Purkait, *J. Hazard. Mater.*, **2009**, 161, 387–395.
- [56] A. Ledesma-Durán, S.I. Hernández, I. Santamaría-Holek, *J. Phys. Chem. C*, **2017**, 121, 14557–14565.
- [57] F. Batool, I. Akbar, Sh. Iqbal, S. Noreen, S.N. Bukhari, *Bioinorg Chem. Appl.*, **2018**, 1–11.
- [58] Q.X. Liu, Y.R. Zhou, M. Wang, *Adsorpt Sci. Technol.*, **2019**, 37, 312–332.
- [59] B.K. Nandi, A. Goswami, M.K. Purkait, *J. Hazard. Mater.*, **2009**, 161, 387–395.
- [60] B.H. Hameed, A.A. Ahmad, *J. Hazard. Master.*, **2009**, 164, 870–875.

How to cite this manuscript: Mohtaram Janighorban, Nahid Rasouli, Nasrin Sohrabi, Mehroang Ghaedi, Response Surface Methodology for Optimizing Cd(II) Adsorption onto a Novel Chemically Changed Nano Zn₂Al-Layer Double Hydroxide, *Adv. J. Chem. A*, **2020**, 3, S701–S721.